PERGAMON

International Journal of Heat and Mass Transfer 45 (2002) 5209–5219

International Journal of HEAT and MASS TRANSFER

www.elsevier.com/locate/ijhmt

Heat transfer and phase change of liquid in an inclined enclosure packed with unsaturated porous media

W. Liu [a,*], S. Shen [a], S.B. Riffat [b]

[a] Department of Power Engineering, Huazhong University of Science and Technology, Wuhan, 430074, China
[b] School of the Built Environment, The University of Nottingham, Nottingham NG7 2RD, UK

Received 8 May 2002

Abstract

In this paper, we present a mathematical model to describe the simultaneous heat and mass transfer with liquid phase change in unsaturated porous media. Two-dimensional natural convective flow in an inclined rectangular enclosure with porous material unsaturated with fluid is analyzed numerically. The parameter variations are considered for the tilted angle, the aspect ratio and the Darcy–Rayleigh number. Local and global Nusselt numbers are presented as functions of those parameters. Compared with the saturated porous material, the heat transfer characters in the unsaturated case are discussed for the identical aspect ratio and Darcy–Rayleigh number, The discussion is also made for the field synergy of fluid velocity and heat flow in natural convection.

Keywords: Porous media; Inclined enclosure; Convection; Phase change; Field synergy

1. Introduction

There are many applications of natural convection in porous media, such as heat storage using porous media, porous media insulation materials, underground diffusion of contaminants, petroleum extraction and electronic cooling. These sorts of applications have motivated an increasing number of investigations on it.

In most practical situations, the flow pattern in porous media would probably be three-dimensional. However, two-dimensional flows do exist both under laboratory conditions and in nature. The understanding from two-dimensional analysis may facilitate the studies on the fully three-dimensional situation. In the present study, we focus on the natural convection in the unsaturated porous media with two-dimensional pattern.

Consider a rectangular enclosure with two opposing walls at constant temperatures separately and the other two walls thermally insulated, which was tilted with respect to the horizontal direction. A lot of theoretical and experimental work dealt with the titled enclosure with porous material. Valsuk [1] determined numerically the heat transfer as a function of the tilted angle and found that the global Nusselt number is maximized at an angle of approximate 50° for Darcy–Reyleigh numbers in the range of 100–350. This effect was also found by Holst and Aziz [2], who investigated a square enclosure saturated by a fluid with temperature-dependent physical properties. Weber [3] investigated the thermal convection in a layer of infinite extension using a perturbation technique. Walch and Dulieu [4] analyzed the convection in slightly inclined two-dimensional cavities and showed that anomalous modes exist for inclinations less 7°. Using analytical and numerical methods, Caltagirone and Bories [5] determined two- and three-dimensional solutions for the inclined box and examined their stability. Experimental work was also conducted by Bories [6,7] and his coworkers. They reported hexagonal cells similar to Bénard–Rayleigh cell for $\boldsymbol{a} < 15°$ and $40 < R < 250$, where $\boldsymbol{a}$ is the tilted angle and R is the Darcy–Rayleigh number. Multiple cells with axes parallel to the

* Corresponding author. Tel.: +86-27-8754-2618; fax: +86-27-8754-0724.
E-mail address: weiliu@public.wh.hb.cn (W. Liu).

0017-9310/02/$ - see front matter
PII: S0017-9310(02)00210-7

Nomenclature

$\boldsymbol{a}$	tilted angle
$\boldsymbol{b}$	included angle between $\widetilde{V}_g$ and $\nabla\Theta$ vectors
c	specific heat, J/(kg K)
Da	Darcy number
D_l	diffusivity of liquid in porous medium, m^2/s
D_v	molecular diffusivity of vapor in air, m^2/s
D_{Tv}	diffusivity due to existence of temperature gradient, $m^2/(s K)$
D_{lv}	diffusivity due to existence of moist content gradient, m^2/s
g	acceleration of gravity, m/s^2
H	height of the porous layer, m
$\boldsymbol{i}$	unit vector
$\boldsymbol{j}$	unit vector
J_a	factor of phase change, dimensionless number
$\boldsymbol{k}$	unit gravitational acceleration vector
k_g	equivalent permeability of gas-mixture, m^2
k_l	unsaturated permeability of liquid, m^2
K_g	infiltrating conductivity of gas-mixture, m/s
K_l	hydraulic conductivity of liquid, m/s
Le	Lewis number
$\dot{m}$	mass rate of phase change, $kg/(m^3 s)$
M	aspect ratio
Nu_m	global Nusselt number
Nu_x	local Nusselt number
P	pressure, Pa
Pr	Prandtl number
R	Darcy–Rayleigh number
S	source term, saturation
t	time, s
T	temperature, K(°C)
u	velocity component in x-direction, m/s
v	velocity component in y-direction, m/s
V	averaging volume, m^3
$\boldsymbol{V}$	velocity vector, m/s
$\boldsymbol{V}_{v,d}$	vapor diffusivity velocity, m/s
W	width of the porous layer, m
X, Y	spatial coordinates, m

Greek symbols

α	thermal diffusivity of fluid, m^2/s
α_m	thermal diffusivity of porous media, m^2/s
β	thermal expansion coefficient, 1/K
γ	latent heat, J/kg
Γ_D	dimensionless number
ε	phase content, %
λ_m	apparent thermal conductivity, W/(m K)
λ	thermal conductivity, W/(m K)
Θ	dimensionless temperature
Λ	dimensionless conductivity
μ	viscosity, kg/(m s)
υ	kinematic viscosity, m^2/s
ρ	density, kg/m^3
ϕ	dimensionless parameter
ω	porosity, %

Subscripts

a	air, ambient
c	cold wall
eff	effective quantities
g	gaseous mixture
h	hot wall
l	liquid
m	apparent mean, mass
s	solid
v	vapor

Superscript

$\sim$	dimensionless quantities

top and bottom walls were found for $40 < R\cos\boldsymbol{a} < 240$. There are no sharply defined boundaries for separating the different modes. Kaneko et al. [8] made experiments by using some kind of sand in the range of $\boldsymbol{a} < 30°$. They reported multiple transversal cells with horizontal axes for $\boldsymbol{a} < 15°$. A single two-dimensional cell appeared for $\boldsymbol{a} > 15°$.

In the above publications, the authors concentrated their studies on the porous media saturated with single fluid. Unsaturated porous media with phase change have received less attention. Compared with the porous media saturated with single fluid, much more physical mechanisms in transport process are involved in the liquid-unsaturated porous media. In the view of the complexity of multi-phase flow and phase change process, Slattery [9] and Whitaker [10] originally developed the averaged-volume method to solve the problem. Based on the thermodynamics principle, Philip and DeVries [11], DeVries [12] and Luikov [13] carried out the excellent work. Bouddor et al. [14] presented a new mathematical model for heat and mass transfer in porous media and tried to take all the complexity of interactions into account. But his mathematical model is too complex to be solved. Minkowyca et al. [15] investigated the phenomena on departure from local thermal equilibrium that is a typical assumption in most studies conducted on multi-phase flow in unsaturated porous media. Some other work [16,17] aimed to analyze the effect of ambient parameters on all field variables was carried out in the confined soil bed with profiling all

variable distributions in two dimension, influenced by the ambient conditions.

The objective of the present study is to analyze numerically the behavior of natural convection flows in a tilted rectangular porous layer unsaturated with liquid-water. The effect of phase change of water has been emphasized. The study is also concerned with the heat transfer characteristics in the porous layer, and the method of field synergy is adopted to describe the mechanism of local heat transfer enhancement.

2. Mathematical formulations

2.1. Theoretical considerations

We have established a model [18] to describe the simultaneous heat, moisture and vapor migration in unsaturated porous media with phase change. The field variables include temperature T, liquid content ε_l, pressure P, liquid velocity $\boldsymbol{V}_l$, gas velocity $\boldsymbol{V}_g$, vapor velocity $\boldsymbol{V}_v$ and phase change rate of evaporation and condensation $\dot{m}$. For the two-dimensional flow, the velocity vectors can be written as

$$\boldsymbol{V}_l = u_l\boldsymbol{i} + v_l\boldsymbol{j}, \quad \boldsymbol{V}_g = u_g\boldsymbol{i} + v_g\boldsymbol{j}, \quad \boldsymbol{V}_v = u_v\boldsymbol{i} + v_v\boldsymbol{j}.$$

Continuity equations

Liquid:

$$\frac{\partial(\varepsilon_l\rho_l)}{\partial t} + \nabla\cdot(\varepsilon_l\rho_l\boldsymbol{V}_l) = -\dot{m} \tag{1}$$

Gas:

$$\frac{\partial(\varepsilon_g\rho_g)}{\partial t} + \nabla\cdot(\varepsilon_g\rho_g\boldsymbol{V}_g) = \dot{m} \tag{2}$$

Vapor:

$$\frac{\partial(\varepsilon_g\rho_v)}{\partial t} + \nabla\cdot(\varepsilon_g\rho_v\boldsymbol{V}_v) = \dot{m} \tag{3}$$

Momentum equations

Liquid phase:

$$\frac{\partial\boldsymbol{V}_l}{\partial t} + \boldsymbol{V}_l\cdot\nabla\boldsymbol{V}_l - \frac{\dot{m}}{\varepsilon_l\rho_l}\boldsymbol{V}_l = -\frac{gD_l}{K_l}\nabla\varepsilon_l - \frac{g\varepsilon_l}{K_l}\boldsymbol{V}_l - \frac{g\varepsilon_g}{K_g}\times(\boldsymbol{V}_l - \boldsymbol{V}_g) - \boldsymbol{g} + \nu_l\nabla^2\boldsymbol{V}_l \tag{4}$$

Gaseous phase:

$$\frac{\partial\boldsymbol{V}_g}{\partial t} + \boldsymbol{V}_g\cdot\nabla\boldsymbol{V}_g + \frac{\dot{m}}{\varepsilon_g\rho_g}\boldsymbol{V}_g = -\frac{1}{\rho_g}\nabla p - \frac{g\varepsilon_g}{K_g}(\boldsymbol{V}_g - \boldsymbol{V}_l) - \boldsymbol{g}\beta(T - T_c) + \nu_g\nabla^2\boldsymbol{V}_g \tag{5}$$

Energy equation

$$(\rho c)_m\frac{\partial T}{\partial t} + ((\rho c)_l\boldsymbol{V}_l + (\rho c)_g\boldsymbol{V}_g + (\rho c)_v\boldsymbol{V}_v)\cdot\nabla T + ((\rho c)_l\boldsymbol{V}_l\cdot\nabla\varepsilon_l + (\rho c)_g\boldsymbol{V}_g\cdot\nabla\varepsilon_g + (\rho c)_v\boldsymbol{V}_v\cdot\nabla\varepsilon_g)T = \lambda_m\nabla^2 T - \dot{m}\gamma + S \tag{6}$$

Some of the characteristics for the above theoretical modeling could be discussed as follows.

(1) The absolute velocity of vapor is defined as $\boldsymbol{V}_v = \boldsymbol{V}_g + \boldsymbol{V}_{v,d}$, and the vapor diffusive velocity is indicated as $\boldsymbol{V}_{v,d} = -D_{Tv}\nabla T - D_{lv}\nabla\varepsilon_l$ [18]. When the quantification relations among diffusive velocity, temperature and vapor phase content are established, we can easily explain the effect of vapor diffusion on the equilibrium of mass and energy. Thus the continuity equation (3) can be taken as a supplement relation contributed to the present model, and the absolute velocity of vapor plays an important role in the energy equation. This may be the good way of adding micromechanism of the molecular diffusivity into macromotion of gaseous phase, through relative relation between $\boldsymbol{V}_l$ and $\boldsymbol{V}_g$ which appears also in the momentum equation.

(2) The Dalton's partial pressure law $P = P_a + P_v$ is introduced in the modeling assumptions (P_a for air partial pressure and P_v for saturated vapor pressure), and the volumetric content relation of $\varepsilon_a = \varepsilon_v = \varepsilon_g$ for air and vapor are satisfied (air and vapor are filled everywhere in the pore-space of porous media). Thus we can reasonably regard that ε_a and ε_v are not independent variables, while ε_g is depended on ε_l which is the only content-independent variable. This treatment may be the key point for us to solve the problem by reducing the variables numbers in the equations.

(3) Based on the fact that $\varepsilon = \varepsilon_s + \varepsilon_l + \varepsilon_g$, the mean physical properties of porous media can be written as $(\rho c)_m = \varepsilon_s(\rho c)_s + \varepsilon_l(\rho c)_l + \varepsilon_g(\rho c)_g$. And also from the principle of constant volume content for gaseous components $\varepsilon_g = \varepsilon_a = \varepsilon_v$, we simply set $(\rho c)_g = \rho_a c_a + \rho_v c_v$. The apparent heat conductivity of the porous material, according to the mean-weighted method, is simply defined as $\lambda_m = \varepsilon_s\lambda_s + \varepsilon_l\lambda_l + \varepsilon_g\lambda_g$.

(4) We could say from the above discussions that, two kinds of physical states (liquid and vapor) and motion manners (macromotion and microdiffusivity) for the moisture in the unsaturated porous material are both considered in the mathematical modeling. Both of the motion rate and the phase-change rate for moisture can be taken into account.

(5) Noting that $K_l = k_l g/\upsilon_l$ and $K_g = k_g g/\upsilon_g$, we had developed an effective formulation to calculate the gaseous infiltrating conductivity K_g [19] corresponding to the liquid hydraulic conductivity K_l, which can demonstrate the mechanisms of Darcy's drag resistance

in terms of gaseous phase and the reaction of liquid to gaseous mixture. It may be rarely considered by others and could be written as

$$K_g = (1-S)^3\left(\frac{1-\omega}{1-\omega(1-S)}\right)^{4/3}\frac{v_l}{v_g}K_l \tag{7}$$

Through such a disposal, we can overcome the difficulty due to lacking of physical property in the gaseous momentum equation, and get reasonable calculation results benefiting from this. Furthermore, it allows us to consider the relative motion between gas and liquid phases by the Darcy's terms both in gas and liquid momentum equations (4) and (5).

(6) As we assume that the liquid vapor in the interstitial space is of the saturated pressure, so that the present model is developed to reflect the evaporation and the condensation in the porous matrix. As a matter of fact, the phase change in the unsaturated porous material acts as an evaporation source some time or a condensation sink some other time, or both of source and sink at the same time in different regions. The sign of field variable $\dot{m}$ could represent the characteristic of source or sink. The contribution of phase change rate $\dot{m}$ has been added into the mass, momentum and energy equations.

From the above discussions, we have explained the present ten-variable equations, in which the momentum equations are very analogous to Navier–Stokes equation, but very different from the Darcy's motion equation. By adding the following expression as a supplemental relation for the model, the equations (1)–(6) can be perfected mathematically.

$$\boldsymbol{V}_v = \boldsymbol{V}_g + \boldsymbol{V}_{v,d} = \boldsymbol{V}_g - D_{Tv}\nabla T - D_{lv}\nabla\varepsilon_l \tag{8}$$

There should be no doubts that the mathematical model under investigation introduces more transport or migration mechanisms in the bed of unsaturated porous material compared with some other models, which improves the theoretical modeling both mathematically and physically.

2.2. Dimensionless model simplification

Consider a rectangular water-unsaturated porous layer as depicted in Fig. 1, where T_1 and T_0 represent the temperature of the hot and the cold walls respectively, while the other two walls are adiabatic. The layer is tilted at an angle with respect to the horizontal plane, and H is units high and W units wide.

Basic assumptions have been made as: (1) Local thermal equilibrium is satisfied throughout the porous media; (2) Gaseous mixture (air plus vapor) in the enclosure can be treated as ideal gas; (3) Partial pressure of vapor is in the equilibrium pressure of saturated state; (4) Boussinesq's approximation is suitable for natural convection in gaseous space; (5) Momentum change rate of liquid is so small that it could be omitted.

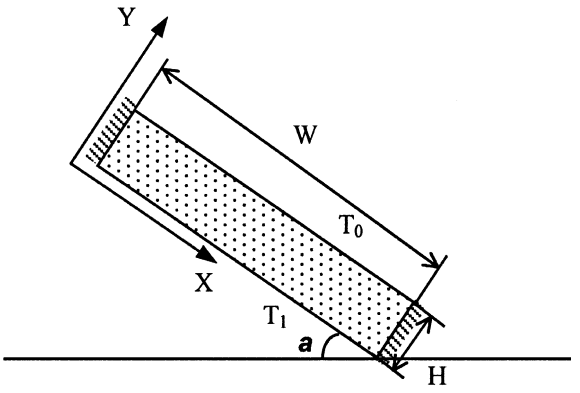

Fig. 1. The tilted porous layer.

In the present investigation, we analyze the steady state, not involving the relative relations between the liquid and the gas phases. To simplify the controlling equations, the dimensionless quantities are defined as

$$\Theta = \frac{T-T_c}{T_h-T_c},\quad \widetilde{P} = \frac{k_g}{\alpha_m\rho_g v_g}P,\quad \widetilde{V}_l = \frac{H}{\alpha_m}\boldsymbol{V}_l,$$

$$\widetilde{V}_g = \frac{H}{\alpha_m}\boldsymbol{V}_g,\quad \widetilde{V}_v = \frac{H}{\alpha_m}\boldsymbol{V}_v,\quad \tilde{m} = \frac{H^2}{\alpha_m}\dot{m},$$

$$Da = \frac{k_g}{H^2},\quad R = \frac{g\beta\Delta T k_g H}{\alpha_m v_g},\quad Pr = \frac{v_g}{\alpha_m},$$

$$Le^* = \frac{\alpha_m}{D_{Tv}}\Delta T,\quad Le^{**} = \frac{\alpha_m}{D_{lv}},\quad \Lambda = \frac{\lambda_g}{\lambda_m},$$

$$\Gamma_D = \frac{D_l}{\alpha_m},\quad \tilde{g} = \frac{H^3}{v_l\alpha_m}g,\quad Ja = \frac{\gamma}{c}\Delta T,$$

$$\phi_l = \frac{(\rho c)_l}{(\rho c)_m},\quad \phi_g = \frac{(\rho c)_g}{(\rho c)_m},\quad \phi_v = \frac{(\rho c)_v}{(\rho c)_m}.$$

The dimensionless equations becomes

$$\nabla(\varepsilon_l\tilde{\rho}_l\widetilde{V}_l) = -\tilde{m} \tag{9}$$

$$\nabla(\varepsilon_g\tilde{\rho}_g\widetilde{V}_g) = \tilde{m} \tag{10}$$

$$\nabla(\varepsilon_g\tilde{\rho}_v\widetilde{V}_v) = \tilde{m} \tag{11}$$

$$\widetilde{V}_l = -\frac{\Gamma_D}{\varepsilon_l}\nabla\varepsilon_l + \frac{Da}{\varepsilon_l}\tilde{g}\boldsymbol{k} \tag{12}$$

$$\frac{Da}{\Lambda Pr}\widetilde{V}_g\cdot\nabla\widetilde{V}_g = -\nabla\widetilde{P} - \varepsilon_g\widetilde{V}_g + \Lambda R\Theta\boldsymbol{k} + Da\nabla^2\widetilde{V}_g \tag{13}$$

$$(\phi_l\widetilde{V}_l + \phi_g\widetilde{V}_g + \phi_v\widetilde{V}_v)\cdot\nabla\Theta = \nabla^2\Theta - Ja\tilde{m} \tag{14}$$

where $\boldsymbol{k} = -\sin\boldsymbol{a}\boldsymbol{i} + \cos\boldsymbol{a}\boldsymbol{j}$ stands for the unit gravitational acceleration vector. The dimensionless equation for vapor diffusivity takes the form as

$$\widetilde{V}_{v,d} = -\nabla\Theta/Le^{*} - \nabla\varepsilon/Le^{**} \tag{15}$$

The non-dimensional boundary conditions are

$$X = 0, \quad \frac{\partial\Theta}{\partial X} = 0, \quad \widetilde{V}_g = \widetilde{V}_l = 0 \tag{16}$$

$$X = 1, \quad \frac{\partial\Theta}{\partial X} = 0, \quad \widetilde{V}_g = \widetilde{V}_l = 0 \tag{17}$$

$$Y = 0, \quad \Theta = 1, \quad \widetilde{V}_g = \widetilde{V}_l = 0 \tag{18}$$

$$Y = 1, \quad \Theta = 0, \quad \widetilde{V}_g = \widetilde{V}_l = 0 \tag{19}$$

$$t = 0, \quad \Theta(X, Y, t) = 0 \tag{20}$$

The non-dimensional stream function of gas phase is defined by

$$\tilde{u}_g = \frac{\partial\Psi}{\partial X}, \quad \tilde{v}_g = -\frac{\partial\Psi}{\partial Y}, \tag{21}$$

The non-dimensional heat transfer coefficient is defined as:

(1) The local Nusselt number

$$Nu_x = \frac{\partial\Theta}{\partial Y} \tag{22}$$

(2) The global Nusselt number

$$Nu_m = \int_0^1 \frac{\partial\Theta}{\partial Y}\,dX \tag{23}$$

3. Numerical analysis and discussion

The difference schemes are selected for the different equations to solve the problem. The center scheme is used for liquid phase and vapor diffusion equations, the upwind scheme is used for Eq. (11), and the hybrid scheme is used for gas phase momentum equations and energy equation. The iterative cycle was repeated until the difference in the global Nusselt number at the hot and cold walls was within 0.1%.

3.1. Convective mode

It should be remarked that we refer to two-dimensional convective motion for the gaseous mixture. An obvious characteristic of natural convection in the saturated porous material is the appearance of single or multiple cells flows [20]. For the present numerical investigation, we observed the similar flow modes for the unsaturated case. Depending on the aspect ratio $M = W/H$, the tilted angle $\boldsymbol{a}$ and the Darcy–Rayleigh number R, single or multiple cells convection can be found. For $M = 1$, $R = 100$ or 40, the single cell mode was obtained in the angle range $0° \leqslant \boldsymbol{a} \leqslant 180°$. Two examples of such flow are given in Figs. 2 and 3 where the streamlines,

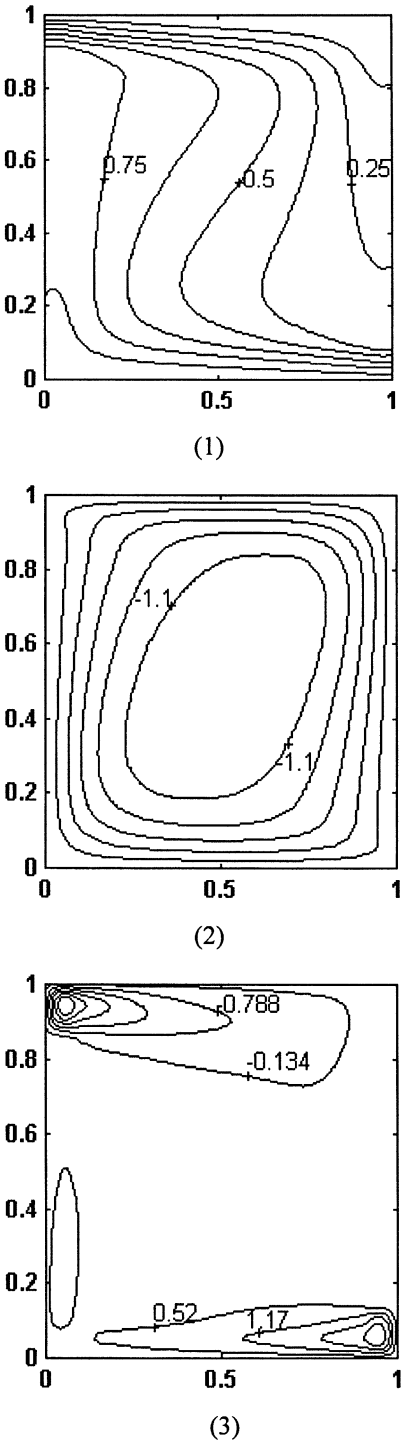

Fig. 2. (1) Isotherms, (2) streamlines and (3) contours of evaporation and condensation rates for $M = 1$, $R = 100$, $\boldsymbol{a} = 30°$.

isotherms and contours of evaporation and condensation rates are shown for $\boldsymbol{a} = 30°$, $R = 100$ and 40 respectively. Figs. 2(2,3) and 3(2,3) show that the magnitudes

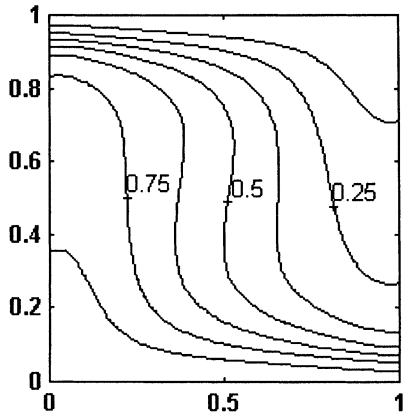

(1)

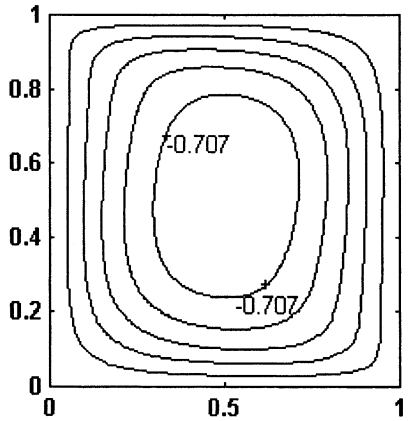

(2)

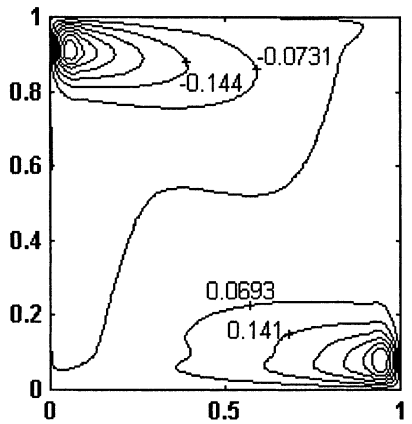

(3)

Fig. 3. (1) Isotherms, (2) streamlines and (3) contours of evaporation and condensation rates for $M = 1$, $R = 40$, $\alpha = 30°$.

of the stream function and the evaporation or condensation rates become larger as R increases, which indicates a more vigorous motion in the porous layer as expected. In Figs. 2(1) and 3(1), we find that heat transfer is more effective at the upper- and lower-most corners where the temperature gradients are greater. This effect can be implied from the deformation of isothermal lines caused by the motion of gaseous mixture with phase change, which is totally different from the conductive pattern.

When aspect ratios are greater than unity, a variety of convective modes appear. For $M = 3$ and a small R, single cell convection takes place for tilted angles larger than 50° approximately. Different multiple-cell flow patterns appear for smaller tilted angles. Typical isotherms and streamlines for $R = 40$ and $\alpha = 45°$, 22.5°, 15° and 0° are shown in Figs. 4–7. Fig. 4 shows a single cell where the gaseous mixture circulates inside the porous layer. Fig. 5 shows a typical convective mode with one main cell plus two secondary cells. As the tilted angle is further reduced to 15°, three clearly isolated cells circulate in the alternate directions. When the porous layer is horizontal, namely $\alpha = 0°$, four cells develop with rotation in the alternate directions.

Concerning the behaviors of evaporation and condensation, we find that they are strongly correlated with the convective mode. When the convective motion takes the form of single cell or a main cell with secondary cells (Figs. 2–5), there are a core of evaporation and a core of condensation appearing at the lower-and upper-most

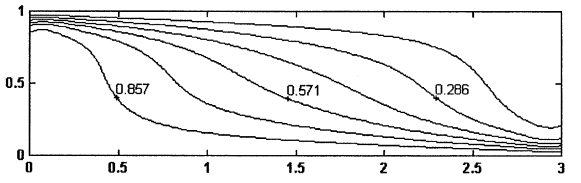

(1)

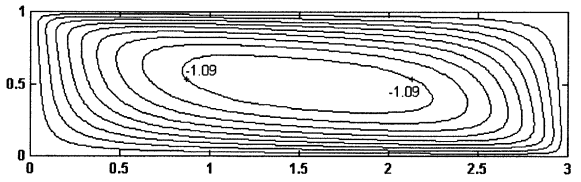

(2)

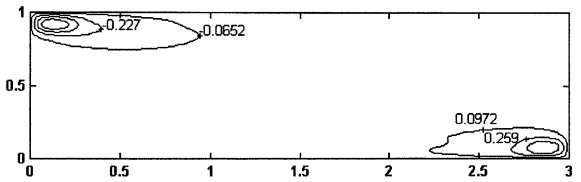

(3)

Fig. 4. (1) Isotherms, (2) streamlines and (3) contours of evaporation and condensation rates for $M = 3$, $R = 40$, $\alpha = 45°$.

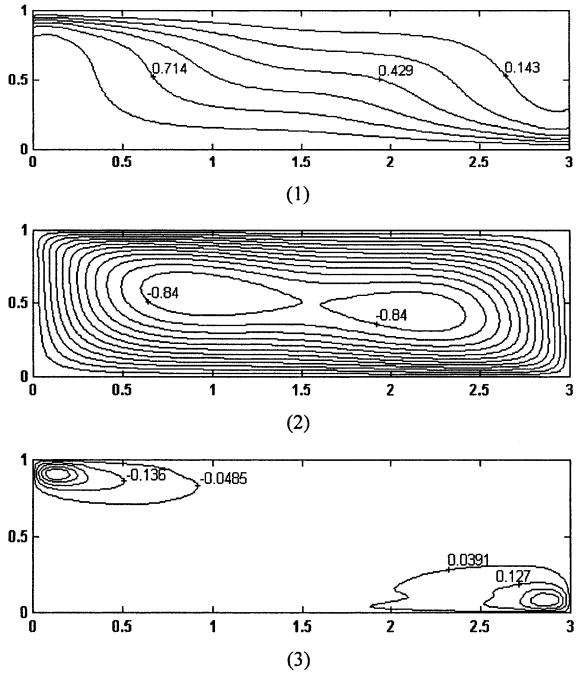

Fig. 5. (1) Isotherms, (2) streamlines and (3) contours of evaporation and condensation rates for $M = 3$, $R = 40$, $\alpha = 22.5°$.

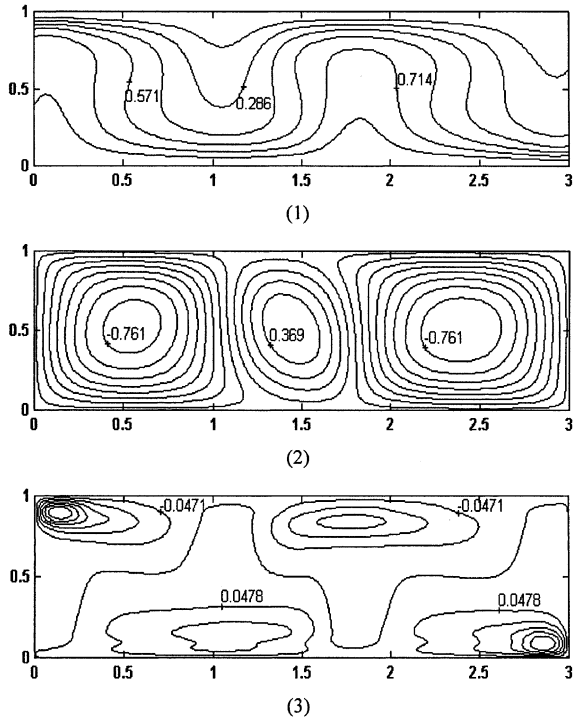

Fig. 6. (1) Isotherms, (2) streamlines and (3) contours of evaporation and condensation rates for $M = 3$, $R = 40$, $\alpha = 15°$.

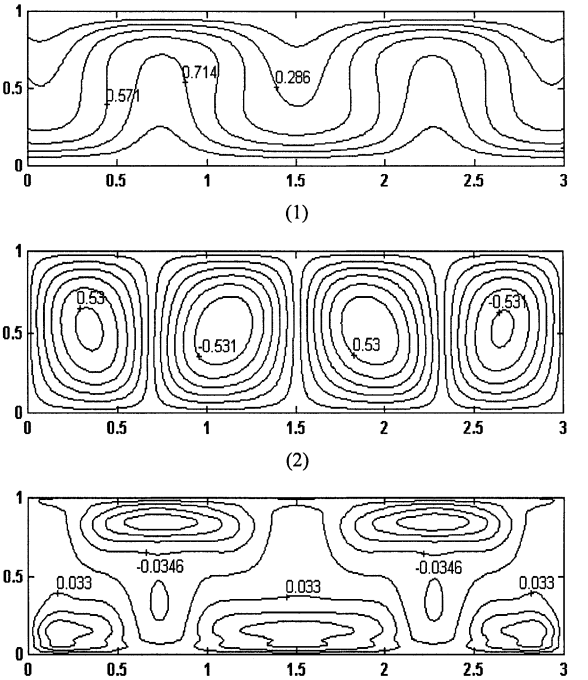

Fig. 7. (1) Isotherms, (2) streamlines and (3) contours of evaporation and condensation rates for $M = 3$, $R = 40$, $\alpha = 0°$.

corners respectively. For multiple-cell flow (Figs. 6 and 7), it can be observed that several cores of evaporation or condensation exist in the vicinity of the hot wall or the cold wall.

3.2. Heat transfer characteristics

We can use the local Nusselt number Nu_x to identify the regions on the wall where heat transfer is more effective. This is shown for the hot wall in Fig. 8 for $R = 40$ and aspect ratio of $M = 3$ and $M = 1$ respectively. It is clearly shown that most of the heat is transferred near the right corners of the porous layer for the single cell mode which corresponds to the curve of $\alpha = 60°$ in Fig. 8(1) and either of curves in Fig. 8(2). When multiple-cell flow presents, which corresponds to the curve of $\alpha = 15°$ in Fig. 8(1), heat transfer is enhanced in the vicinity of curve peaks. Although the curve of Nu_x for $M = 3$ and $\alpha = 15°$ fluctuates in the X-direction, it is found that the presence of multiple-cell mode has the overall effect of increasing heat transfer, as shown in Fig. 10.

The phenomena of synergy between the fluid velocity and the heat flow field for convective heat transfer [21,22] can well explain the local heat transfer enhancement here. Noting that the velocity vector $\widetilde{V}_g$ and the temperature gradient $\nabla\Theta$ are two essential factors

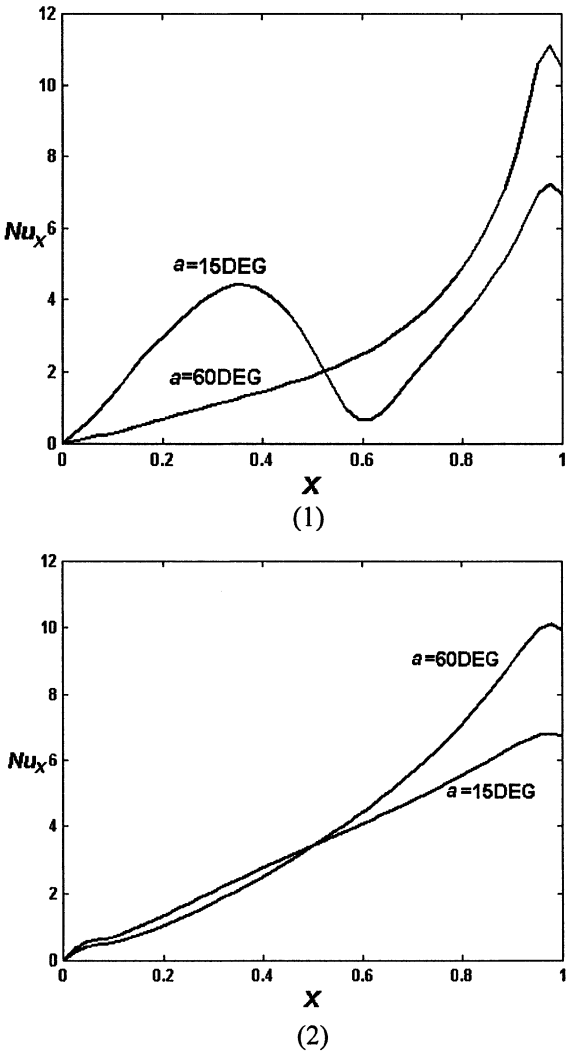

Fig. 8. Variations of the Nusselt numbers with X for (1) $R = 40$, $M = 3$ and (2) $R = 40$, $M = 1$.

dominating the heat convection, for the flow near the hot wall of the porous layer (see Fig. 1), the variations of the product of the absolute values $|\widetilde{V}_g| \cdot |\nabla\Theta|$, the included angle $\boldsymbol{b}$ between vectors $\widetilde{V}_g$ and $\nabla\Theta$, and the local Nusselt number Nu_x in the X-direction are shown in Figs. 9 and 10 for $\boldsymbol{a} = 30°$ and $R = 100$ with $M = 1$ and 3 respectively. We arbitrarily choose two points A and B along the cross-section of porous layer near the wall to let $|\widetilde{V}_g| \cdot |\nabla\Theta|(A) = |\widetilde{V}_g| \cdot |\nabla\Theta|(B)$ shown in Fig. 9(1). There should be the counterparts for A and B in Fig. 9(2–3), namely A′ and A″ corresponding to A, B′ and B″ to B. Their geometry positions meet $X(A') = X(A'') = X(A)$ and $X(B') = X(B'') = X(B)$. It can be observed that when the product $|\widetilde{V}_g| \cdot |\nabla\Theta|(A) = |\widetilde{V}_g| \cdot |\nabla\Theta|(B)$, the included angle $\boldsymbol{b}(A') > \boldsymbol{b}(B')$, but the local Nusselt number $Nu_x(A'') < Nu_x(B'')$. Likewise, we find

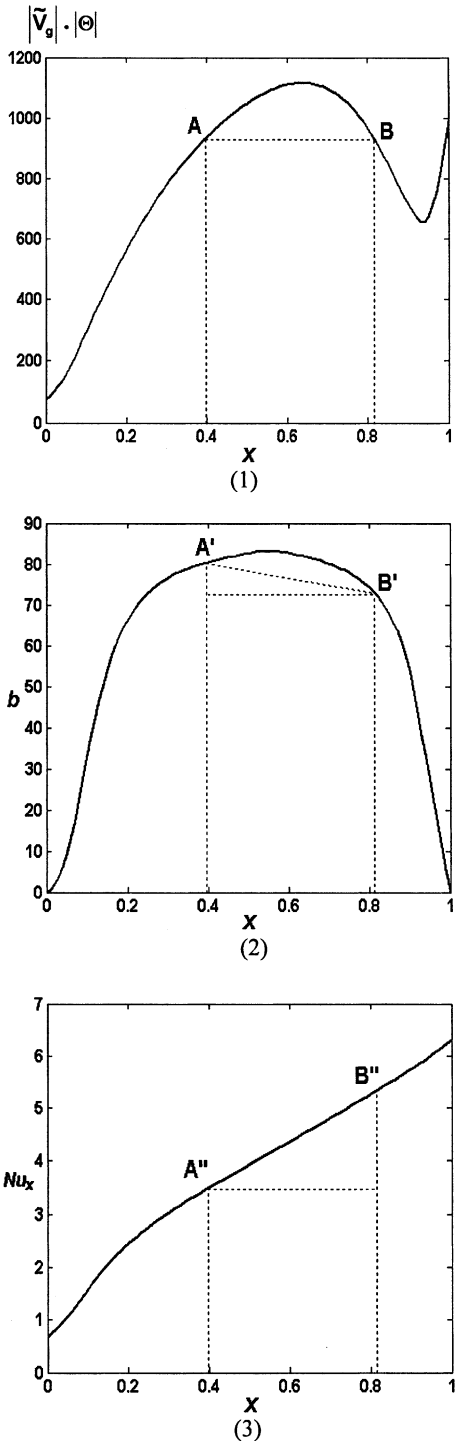

Fig. 9. Variations of $|\widetilde{V}_g| \cdot |\nabla\Theta|$, $\boldsymbol{b}$ and Nu_x with X for $R = 100$, $\boldsymbol{a} = 30°$ and $M = 1$.

when $|\widetilde{V}_g| \cdot |\nabla\Theta|(C) = |\widetilde{V}_g| \cdot |\nabla\Theta|(D)$, $\boldsymbol{b}(C') > \boldsymbol{b}(D')$ but $Nu_x(C'') < Nu_x(D'')$ in Fig. 10. Although we only enu-

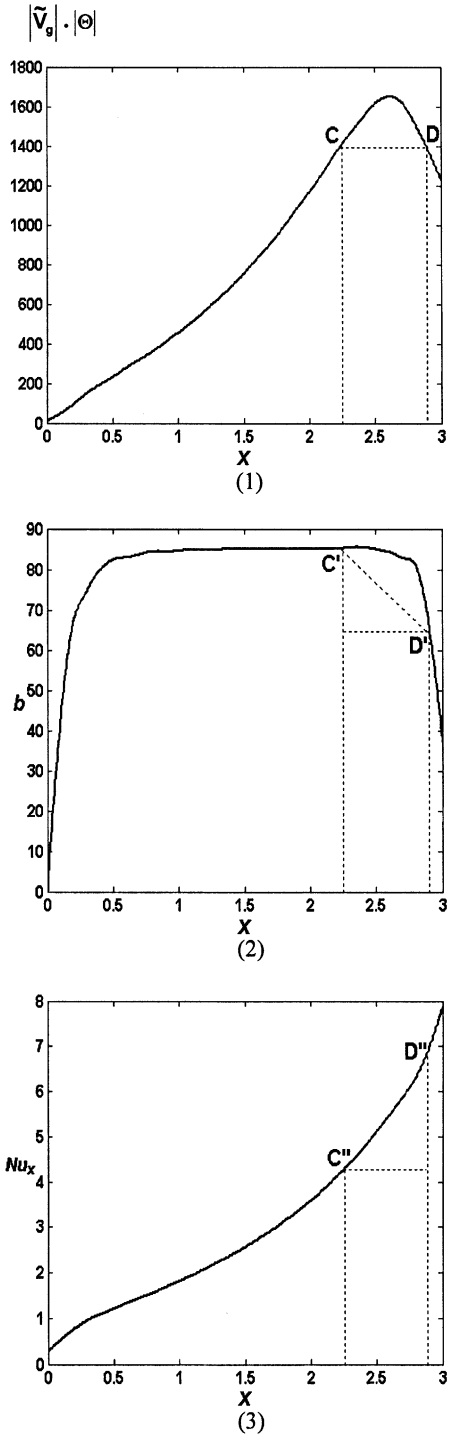

Fig. 10. Variations of $|\widetilde{V}_g| \cdot |\nabla\Theta|$, $\boldsymbol{b}$ and Nu_x with X for $R = 100$, $\boldsymbol{a} = 30°$ and $M = 3$.

merate two examples for $\boldsymbol{a} = 30°$, the similar results have been obtained for different $\boldsymbol{a}$, with any R and M. It can be seen that the local Nusselt number depends not only on the absolute values of vectors $\widetilde{V}_g$ and $\nabla\Theta$, but also on their angle $\boldsymbol{b}$. The smaller the included angle, the greater the heat transport rate for the range of $\boldsymbol{b} < 90°$.

The global Nusselt number Nu_m for $M = 1$, $M = 3$, $R = 100$ and $R = 40$ in the cases of saturated and unsaturated porous media are shown in Fig. 11 as the functions of the tilted angle $\boldsymbol{a}$. The curves of unit aspect ratio show a single maximum at the tilted angle about 50°. However, the curves of aspect ratio $M = 3$ feature several local maxima. For the unsaturated case with $M = 3$ and $R = 100$, the first maximum is at $\boldsymbol{a} = 15°$, and the second one at the tilted angle of 70° approximately. For the situation of $M = 3$ and $R = 40$, the first maximum is at $\boldsymbol{a} = 0°$, the second one at $\boldsymbol{a} = 15°$ and the third one at $\boldsymbol{a} = 70°$ approximately. In the Fig. 11(2) for saturated porous layer, the appearance of single

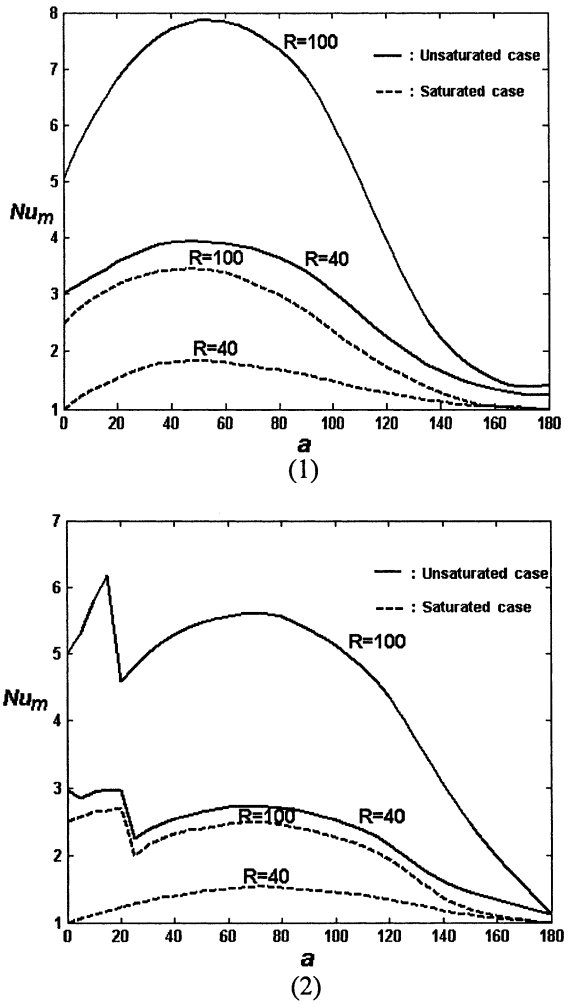

Fig. 11. Variations of the global Nusselt numbers with $\boldsymbol{a}$ for (1) $M = 1$ and (2) $M = 3$.

maximum in the curve at the tilted angle about 70° for aspect ratio $M = 3$ and $R = 40$ can be explained by a single cell flow, which is very analogous to the case of unit aspect ratio. However, the appearance of several peaks in the curves for $M = 3$ and $R = 100$ or 40 should have the geometry characteristics for aspect ratio greater than unity, which is due to the convection with multiple cells.

It is also shown in Fig. 11 that the overall heat transfer in porous layer is very sensitive to the magnitudes of M, $\boldsymbol{a}$ and R. The global Nusselt number may be expressed in terms of $Nu_m = f(M, \boldsymbol{a}, R)$. However, we can impressively observe from Fig. 11 that for the identical R and M, the curves of Nu_m in the unsaturated case is higher than those in the saturated case. In the titled porous layer unsaturated with flow fluid, although the global Nusselt number may be still described as a function of the variables M, $\boldsymbol{a}$ and R, those variables influence not only the flow patterns of the fluid but also the behaviors of evaporation and condensation. Besides the heat conduction and the heat convection, the phase change of the liquid plays an important role in the heat transport process in the enclosure with porous media. Heat transfer is enhanced because of the phase change in the unsaturated porous layer.

4. Conclusions

The natural convection in a two-dimensional porous layer unsaturated with fluid was numerically investigated. Depending on the aspect ratio M, the Darcy–Rayleigh number R and the tilted angle $\boldsymbol{a}$, single cell or multiple-cell convection can take place, which demonstrates convective flow patterns.

For the different flow patterns that may influence the behavior of phase change of liquid, there exists the peak value for global Nusselt number with the change of tilted angle for different aspect ratio M. The multiple-cell convection obviously enlarges the heat transfer through the porous layer. It can be concluded that the overall heat transfer performance for the porous layer unsaturated with liquid is much better than that for the saturated one.

The phenomena of synergy between the fluid velocity and heat flow field have been observed for convective heat transfer in an inclined rectangular enclosure packed with unsaturated porous media. It was found that at arbitrary two points along porous layer near the wall, the smaller is the included angle between the velocity vector and the heat flow vector, the greater the heat transport rate becomes. Therefore, the intensity of convective heat transfer depends not only on the fluid velocity and its properties as expected, but also on the included angle of velocity and temperature gradient vectors, which dominates the local heat transfer rate.

Acknowledgements

The work in the present paper is supported by the National Natural Science Foundation of China (No. 59976010), the National Key Development Program of China for Fundamental Research (No. G2000026303) and the Doctoral Foundation of Ministry of Education, China (No. 2000048731).

References

[1] M.P. Vlasuk, Heat transfer with natural convection in permeable porous medium, 4th All-Union Heat Transfer Conf., Minsk, 1972.
[2] P.H. Holst, K. Aziz, A theoretical and experimental study of natural convection in a confined porous medium, Can. J. Chem. Eng. 50 (1972) 232–241.
[3] J.E. Weber, Thermal convection in a tilted porous layer, Int. J. Heat Mass Transfer 18 (1975) 474–475.
[4] J.P. Walch, B. Dulieu, Convection de Rayleigh–Bénard dans une cavité poruse faiblement inclinée, J. Phys. Lett. Paris 43 (1982) 103–107.
[5] J.P. Caltagirone, S.A. Bories, Solutions and stability criteria of natural convective flow in an inclined porous layer, J. Fluid Mech. 155 (1985) 267.
[6] M.A. Combarnous, S.A. Bories, Hydrothermal convection in saturated porous media, Adv. Hydrosci. 10 (1975) 231–307.
[7] S.A. Bories, M.A. Combarnous, Natural convection in a sloping porous layer, J. Fluid Mech. 57 (1973) 63–79.
[8] T. Kaneko, M.F. Mohtadi, K. Aziz, An experimental study of natural convection in inclined porous media, Int. J. Heat Mass Transfer 17 (1974) 485–496.
[9] J.C. Slattery, Two-phase flow through porous media, AIChE J. 16 (1970) 345–354.
[10] S. Whitaker, Simultaneous heat mass and momentum transfer in porous media a theory of drying, in: Advances in Heat Transfer, Academic Press, New York, 1977.
[11] J.R. Philip, D.A. DeVries, Moisture movement in porous materials under temperature gradients, Trans. Am. Geophys. Union 38 (1957) 222–232.
[12] D.A. DeVries, Simultaneous transfer of heat and moisture in porous media, Trans. Am. Geophys. Union 39 (1958) 909–916.
[13] A.V. Luikov, System of differential equation of heat and mass transfer in capillary porous-bodies, Int. J. Heat Mass Transfer 18 (1975) 1–14.
[14] A. Bouddor et al., Heat and mass transfer in wet porous media in presence of evaporation–condensation, Int. J. Heat Mass Transfer 41 (1998) 2263–2277.
[15] W.J. Minkowycz, Haji-Sheikh, K. Vafai, On departure from local thermal equilibrium in porous media due to a rapidly changing heat source: the Sparrow number, Int. J. Heat Mass Transfer 42 (1999) 3373–3385.
[16] W. Liu, X.X. Zhao, K. Mizukami, 2D numerical simulation for simultaneous heat, water and gas migration in soil bed under different environmental conditions, Heat Mass Transfer 34 (1998) 307–316.
[17] W. Liu, X.X. Zhao, K. Mizukami, Numerical simulation of heat and mass transfer in soil, in: Proceedings of the

10th International Symposium on Transport Phenomena, Japan, 1997.

[18] W. Liu, S.W. Peng, K. Mizukami, A general mathematical modeling for heat and mass transfer in unsaturated porous media: an application to free evaporative cooling, Heat Mass Transfer 31 (1995) 49–55.

[19] W. Liu, S.W. Peng, K. Mizukami, Moisture evaporation and migration in thin porous packed bed influenced by ambient and operative conditions, Int. J. Energ. Res. 21 (1997) 41–53.

[20] S.L. Moya, E. Ramos, M. Sen, Numerical study of natural convection in a tilted rectangular porous material, Int. J. Heat Mass Transfer 30 (1987) 741–756.

[21] Z.Y. Guo, D.Y. Li, B.X. Wang, A novel concept for convective heat transfer enhancement, Int. J. Heat Mass Transfer 40 (1998) 2221–2225.

[22] Z.Y. Guo, S. Wang, Novel concept and approaches of heat transfer enhancement, in: P. Cheng (Ed.), Proceedings of Symposium on Energy and Engineering, Begell House, New York, 2000, pp. 118–126.